Is Complexity Always Better? A Comparative Evaluation of Classical PID and Data-Driven MPC

Jean Pierre Arteaga[1], Juan Francisco Durán[2], and Luis Ismael Minchala[3],

Abstract— **This work presents a structured comparison between classical and data-driven control strategies, focusing on the performance trade-offs associated with model complexity. A PID controller tuned using the Simple Internal Model Control methodology is evaluated against a Model Predictive Control (MPC) approach based on the Koopman operator. The study is conducted on two representative nonlinear multivariable systems: a thermal laboratory platform implemented in a real experimental setup and a simulated multi-tank system. Both control strategies are assessed under equivalent operating conditions using standardized performance indices. The results show that, in systems with relatively simple dynamics, the classical PID controller achieves superior performance across all evaluated metrics. In contrast, for systems with stronger coupling and more complex dynamics, the predictive controller demonstrates advantages in managing time-dependent error, although not consistently outperforming the classical approach in all criteria. These findings highlight that control performance is not solely determined by algorithmic complexity, but strongly depends on system characteristics and evaluation criteria. In this context, this study provides evidence that well-designed classical controllers remain competitive alternatives to advanced data-driven methods.**

I. Introduction

Currently, two well-defined trends can be identified in the development of solutions in control engineering: classical control and data-driven approaches. Within the framework of classical control, several authors [1], [2] have proposed strategies based on the decomposition of complex systems into tractable control structures, such as cascade control, feedforward control, and advanced PID controllers. These approaches stand out for their robustness and ease of implementation in industrial applications, as they rely primarily on process feedback and less on highly optimized models. In this context, it has been argued that simple solutions should be considered as a first option, resorting to more complex methods when classical approaches are not sufficient. In particular, the Simple Internal Model Control (SIMC) approach has been widely used as a systematic methodology for PID controller design, becoming one of the most influential tools in process control.

In contrast, recent developments in modeling complex systems have been driven by data-driven approaches. The increasing availability of process data, together with greater computational capabilities and more efficient training methods, has fostered the use of data-driven techniques to represent the behavior of industrial systems. In this context, surrogate models have been proposed as an alternative to approximate complex physical models or computationally expensive simulations, enabling the capture of input–output relationships with reduced computational cost and facilitating tasks such as optimization, analysis, and control [3]. These approaches allow nonlinear dynamics to be represented through linear models in higher-dimensional spaces, as in the framework of the Koopman operator theory [4]. This representation enables the application of control strategies, such as MPC, which are widely used in industrial processes due to their ability to handle constraints and anticipate the future dynamic behavior of the system.

Despite these advances, a fundamental question arises: to what extent do classical control methods remain competitive compared to modern data-driven approaches? Although the literature includes comparisons between conventional and advanced control strategies, several authors have pointed out important limitations in how these evaluations are carried out. In particular, many studies lack standardized evaluation criteria that allow for an objective comparison between classical and advanced controllers, making it difficult to draw clear conclusions about their relative performance [5]. Similarly, it has been noted that comparisons between model-based methods and data-driven approaches strongly depend on the study conditions and controller configuration, which may lead to biased evaluations when the test scenarios or models do not adequately represent real operating conditions. Furthermore, data-driven identification methods may be limited when the available data are scarce or not representative of the actual system behavior [6]. Moreover, the application of data-driven or simulation-based models to real-world systems remains challenging due to model uncertainty and unmodeled disturbance [7]. In this context, it is necessary to offer an objective evaluation of the relative performance between well-designed classical control strategies and modern data-driven approaches, particularly in nonlinear MIMO systems, where the adoption of more complex strategies over classical methods is not always justified, given that well-tuned classical controllers can provide comparable performance with lower implementation complexity.

In recent years, several works have explored the use of the Koopman theory to obtain linear representations of nonlinear systems to design predictive controllers based on data. Nevertheless, relatively few works evaluate these strategies

[1]Jean Arteaga is with the Research Group on Mechatronics Systems, Universidad Politécnica Salesiana, Cuenca, Ecuador. arteaga@ups.edu.ec

[2]Juan F. Durán is with the Department of Industrial Engineering, Università di Trento, Via Sommarive, 38123 Trento, Italy. juan.duransiguenza@unitn.it

[3]Luis I, Minchala is with the Department of Electrical Engineering, Electronics, and Telecommunications, Universidad de Cuenca, Cuenca, Ecuador ismael.minchala@ucuenca.edu.ec

on real experimental platforms under comparable conditions and uniform evaluation criteria.

In this context, this work presents a structured comparison between a PID controller tuned using SIMC and an MPC strategy based on dynamic models obtained through Koopman Extended Dynamic Mode Decomposition (E-DMD). The comparison is carried out on two representative platforms of nonlinear processes commonly used as benchmarks in process control: the TCLab thermal system, and a simulated multi-tank system. Both systems exhibit nonlinear MIMO dynamics and allow the evaluation of control performance under different dynamic conditions.

The comparison considers: (1) two nonlinear MIMO platforms, (2) different operating scenarios, and (3) the evaluation of performance metrics such as IAE, ITAE, and ISE.

In addition, a critical discussion is presented on the relationship between method complexity and achieved performance, providing evidence that a properly designed PID controller can remain a competitive alternative in certain process control scenarios.

II. Background

A. Conventional modeling and control

In the analysis and control of industrial processes, it is common to start from models derived from physical principles, leading to differential equations that describe the system dynamics. These equations typically exhibit nonlinear behavior due to inherent physical phenomena. However, for control design purposes, it is common to work with linear representations of such systems.

A common approach consists of linearizing the nonlinear model around an operating point or equilibrium using a first-order Taylor expansion [8]. In situations where the complete physical model is not available or is too complex, graphical identification methods can be used to approximate the dominant dynamics of the process using low-order models.

Additionally, even when a transfer function of the system is available, it may not directly satisfy the structure required by SIMC tuning rules, for example due to the presence of zeros in the numerator or additional dynamics not considered in the standard model. In such cases, it is common to approximate the original model using first- or second-order representations with time delay, employing graphical methods to obtain a compatible structure that allows systematic application of tuning rules.

Once a linear representation of the system is available, it is possible to analyze the interaction between variables in multivariable processes. The Relative Gain Array (RGA) is a widely used tool to evaluate the degree of coupling between system inputs and outputs and to determine suitable pairings between manipulated and controlled variables.

In this context, the PID controller in series form can be expressed as

$$C(s) = K_c \left(\frac{\tau_I s + 1}{\tau_I s} \right) (\tau_D s + 1) \tag{1}$$

where K_c is the proportional gain, τ_I is the integral time constant, and τ_D is the derivative time constant.

SIMC rules provide a systematic way to obtain controller parameters from models with dominant delay. For first-order processes with time delay, the model can be written as

$$g(s) = \frac{k\, e^{-\theta s}}{\tau_1 s + 1}, \tag{2}$$

while for second-order processes with time delay, the following representation is used

$$g(s) = \frac{k\, e^{-\theta s}}{(\tau_1 s + 1)(\tau_2 s + 1)}. \tag{3}$$

From these models, the PID controller parameters are obtained through explicit tuning rules [1]. In both cases, the proportional gain is calculated as

$$K_c = \frac{1}{k} \frac{\tau_1}{\tau_c + \theta}, \tag{4}$$

while the integral time is defined as

$$\tau_I = \min\{\tau_1,\, 4(\tau_c + \theta)\}, \tag{5}$$

and the derivative time depends on the model order. For first-order processes, $\tau_D = 0$, while for second-order processes it is given by $\tau_D = \tau_2$.

In these expressions, τ_c is the tuning parameter that defines the trade-off between speed and robustness in the closed-loop system [9], [10]. Smaller values of τ_c lead to faster responses, while larger values increase robustness to uncertainty and noise.

B. Data-driven modeling and predictive control

An alternative to model-based approaches consists of constructing dynamic representations directly from experimental data. These approaches, known as data-driven methods, aim to approximate system behavior using information obtained from measured input–output trajectories [11].

In discrete time, a controlled nonlinear system can be generally represented as

$$\mathbf{x}_{k+1} = F(\mathbf{x}_k, \mathbf{u}_k) \tag{6}$$

where $\mathbf{x}_k \in \mathbb{R}^n$ is the state vector and $\mathbf{u}_k \in \mathbb{R}^m$ is the input vector at time step k. Within this framework, the Koopman operator provides a theoretical formulation to represent nonlinear systems through a linear evolution in a higher-dimensional space of observables. Its practical approximation using EDMD allows obtaining a lifted linear predictor of the form

$$\mathbf{z}_{k+1} = \mathbf{A}_z \mathbf{z}_k + \mathbf{B}_z \mathbf{u}_k, \qquad \hat{\mathbf{x}}_k = \mathbf{C}_z \mathbf{z}_k \tag{7}$$

where $\mathbf{z}_k \in \mathbb{R}^N$ is the lifted state vector, $\mathbf{A}_z$ and $\mathbf{B}_z$ are the identified system matrices in the lifted space, and $\mathbf{C}_z$ is the output reconstruction matrix [12].

Once this model is obtained, it can be used within an MPC framework, where the control action is computed by solving a constrained optimization problem at each sampling instant over a finite prediction horizon. In its standard form, the cost function is written as

$$J = \sum_{k=0}^{N_p} \big(\hat{\mathbf{y}}_k - \mathbf{r}_k\big)^\top \mathbf{Q} \big(\hat{\mathbf{y}}_k - \mathbf{r}_k\big) + \Delta\mathbf{u}_k^\top \mathbf{R}\, \Delta\mathbf{u}_k \tag{8}$$

subject to box constraints on inputs and their increments,

$$\mathbf{u}_{\min} \le \mathbf{u}_k \le \mathbf{u}_{\max}, \qquad \Delta\mathbf{u}_{\min} \le \Delta\mathbf{u}_k \le \Delta\mathbf{u}_{\max} \tag{9}$$

where $\mathbf{Q} \ge 0$ and $\mathbf{R} > 0$ are output and input weighting matrices, respectively [13].

The comparison carried out in this work addresses two different control philosophies:

- structured simplicity;
- data-driven modeling for predictive control.

III. Methodology

This section describes the systems used for experimentation, the derivation of their models for conventional controller design, the formulation of the Koopman-EDMD-based predictive approach, and the setup used to compare both strategies.

A. TCLab

The TCLab system was modeled using energy balances that consider convective and radiative heat transfer with the environment, as well as thermal coupling between both heaters [14]. The nonlinear model can be expressed as in (10) and (11), where the physical parameters of the system are summarized in Table I.

$$\begin{aligned} mc_p \frac{dT_1}{dt} &= UA(T_\infty - T_1) + \epsilon\sigma A(T_\infty^4 - T_1^4) \\ &\quad + UA_s(T_2 - T_1) + \epsilon\sigma A_s(T_2^4 - T_1^4) + \alpha_1 Q_1, \end{aligned} \tag{10}$$

$$\begin{aligned} mc_p \frac{dT_2}{dt} &= UA(T_\infty - T_2) + \epsilon\sigma A(T_\infty^4 - T_2^4) \\ &\quad - UA_s(T_2 - T_1) - \epsilon\sigma A_s(T_2^4 - T_1^4) + \alpha_2 Q_2. \end{aligned} \tag{11}$$

By imposing steady-state conditions on (10) and (11), the equilibrium points were obtained as

$$T_{1e} = 336.79\,K \;\; (63.64°C) \qquad T_{2e} = 324.97\,K \;\; (51.82°C)$$

From these values, Jacobian linearization yielded the local state-space model $\dot{\mathbf{x}} = \mathbf{A}\mathbf{x} + \mathbf{B}\mathbf{u}$, from which the transfer matrix $\mathbf{G}(s) \in \mathbb{R}^{2\times 2}$ was obtained as

$$\mathbf{G}(s) = \frac{1}{d(s)} \begin{bmatrix} 0.005s + 4.78\times10^{-5} & 1.474\times10^{-5} \\ 2.164\times10^{-5} & 0.00375s + 3.88\times10^{-5} \end{bmatrix} \tag{12}$$

where $d(s) = s^2 + 0.02s + 8.23\times10^{-5}$.

From the steady-state gains of (12), the static gain matrix $\mathbf{K}$ was constructed and the RGA was computed, yielding

$$\mathbf{RGA} = \begin{bmatrix} 1.2067 & -0.2067 \\ -0.2067 & 1.2067 \end{bmatrix}, \tag{13}$$

TABLE I

Thermal process parameters

Variable	Value
Initial & Ambient temperature (T_0, T_∞)	$296.15\,K$ $(23°C)$
Heater 1 & 2 inputs (Q_1, Q_2)	$0 - 100\,\%$
Heating factor 1 (α_1)	$0.01\,W/\%$
Heating factor 2 (α_2)	$0.0075\,W/\%$
Heat capacity (C_p)	$500\,J/(kg\,K)$
Surface area (A)	$1.0\times10^{-3}\,m^2$ $(10\,cm^2)$
Area between heaters (A_s)	$2\times10^{-4}\,m^2$ $(2\,cm^2)$
Mass (m)	$0.004\,kg$ $(4\,g)$
Heat transfer coefficient (U)	$4.285\,W/(m^2K)$
Emissivity (ϵ)	0.9
Stefan–Boltzmann constant (σ)	$5.67\times10^{-8}\,W/(m^2K^4)$

which indicates that the most suitable pairings for decentralized control are T_1–Q_1 and T_2–Q_2, since the diagonal elements are close to unity and the off-diagonal elements are small.

Since the original transfer functions do not directly match the structure required by SIMC tuning rules, the transfer functions in (12) were approximated using the Smith graphical method, in order to obtain low-order models compatible with this design approach.

$$G_{11}(s) = \frac{0.581811\,e^{-s}}{(116.113794\,s+1)(1.184958\,s+1)}, \tag{14}$$

$$G_{22}(s) = \frac{0.472474\,e^{-s}}{(124.962135\,s+1)(1.275257\,s+1)}. \tag{15}$$

Applying the SIMC tuning rules to (14) and (15), using a tuning parameter of $\tau_c = 100$, the PID controller parameters in parallel form were obtained. For the T_1-Q_1 loop, the resulting parameters were $K_p = 1.9961$, $T_i = 117.2988$, and $T_d = 1.1730$. Similarly, for the T_2-Q_2 loop, the parameters were $K_p = 2.6454$, $T_i = 126.2374$, and $T_d = 1.2624$.

B. Multitank System

The multitank system was modeled using mass balances in two hydraulically coupled tanks and three proportional valves [4], [15], whose openings were normalized in the interval $[0, 1]$. The nonlinear dynamics are given by

$$A_1 \frac{dh_1}{dt} = u_1 q_0 - u_2 a_2 \sqrt{2gh_1}, \tag{16}$$

$$A_2 \frac{dh_2}{dt} = u_2 a_2 \sqrt{2gh_1} - u_3 a_3 \sqrt{2gh_2} \tag{17}$$

where the physical parameters are summarized in Table II. For linearization, the operating point was selected as

$$u_{1e} = u_{2e} = u_{3e} = 0.5 \quad h_{1e} = 0.1181\,m \quad h_{2e} = 0.1070\,m$$

From (16) and (17), Jacobian linearization yielded the local state-space model $\dot{\mathbf{x}} = \mathbf{A}\mathbf{x} + \mathbf{B}\mathbf{u}$, from which the transfer matrix $\mathbf{G}(s) \in \mathbb{R}^{2\times 3}$ was obtained as

TABLE II

MULTITANK SYSTEM PARAMETERS

Variable	Value
Valve 1, 2, 3 opening (u_1, u_2, u_3)	$0 \leq u_{1,2,3} \leq 1$
Valve 2 outlet area (a_2)	$4.380 \times 10^{-5}\, m^2$
Valve 3 outlet area (a_3)	$4.601 \times 10^{-5}\, m^2$
Tank 1 cross-sectional area (A_1)	$0.04\, m^2$
Tank 2 cross-sectional area (A_2)	$0.04\, m^2$
Nominal inlet flow (q_0)	$6.667 \times 10^{-5}\, m^3/s$
Gravitational acceleration (g)	$9.81\, m/s^2$

$$\mathbf{G}(s) = \begin{bmatrix} \dfrac{0.001667}{s+0.003529} & \dfrac{-0.001667}{s+0.003529} & 0 \\ \dfrac{5.881 \times 10^{-6}}{d_2(s)} & \dfrac{0.001667s}{d_2(s)} & \dfrac{-0.001667}{s+0.003894} \end{bmatrix} \tag{18}$$

where $d_2(s) = s^2 + 0.007422s + 1.374 \times 10^{-5}$.

Since the system is non-square (2 outputs, 3 inputs), the RGA was evaluated on 2×2 subsets by excluding one valve at a time. Excluding valve 1 or valve 2 yields $\mathbf{RGA} = \mathbf{I}_{2\times 2}$, while excluding valve 3 gives $\mathbf{RGA} = \left[\begin{smallmatrix} 0 & 1 \\ 1 & 0 \end{smallmatrix}\right]$, indicating that valve 2 governs level h_1 and valve 3 governs h_2; these pairings define the decentralized control structure.

Using a closed-loop tuning parameter of $\tau_c = 60$ and a time-delay parameter of $\theta = 1\,\mathrm{s}$, the resulting PI controller parameters were obtained. For $G_{11}(s)$, the parameters were $K_p = 9.834$, $T_i = 244$; for $G_{12}(s)$, the parameters were $K_p = -9.834$, $T_i = 244$; and for $G_{23}(s)$, the parameters were $K_p = -9.834$, $T_i = 244$.

C. Koopman-EDMD-Based MPC Design

The predictive controller is grounded on a finite-dimensional approximation of the Koopman operator obtained via EDMD [4]. Given a dataset of M state–input–successor triples, the snapshot matrices are arranged as

$$\mathbf{X} = [\mathbf{x}_1 \ \cdots \ \mathbf{x}_M], \ \ \mathbf{X}^+ = [\mathbf{x}_2 \ \cdots \ \mathbf{x}_{M+1}], \ \ \mathbf{U} = [\mathbf{u}_1 \ \cdots \ \mathbf{u}_M]. \tag{19}$$

A dictionary of observable functions $\mathbf{\Phi} : \mathbb{R}^n \times \mathbb{R}^m \to \mathbb{R}^N$ maps each state–input pair to a lifted vector $\mathbf{z}_k = \mathbf{\Phi}(\mathbf{x}_k, \mathbf{u}_k)$. Applying $\mathbf{\Phi}$ column-wise yields the lifted data matrices $\mathbf{Z} = \mathbf{\Phi}(\mathbf{X}, \mathbf{U})$ and $\mathbf{Z}^+ = \mathbf{\Phi}(\mathbf{X}^+, \mathbf{U})$. The EDMD regression problem finds $[\mathbf{A}_z \ \mathbf{B}_z]$ by solving

$$\min_{\mathbf{A}_z, \mathbf{B}_z} \left\| \mathbf{Z}^+ - \mathbf{A}_z \mathbf{\Psi}(\mathbf{X}) - \mathbf{B}_z \mathbf{U} \right\|_F^2, \tag{20}$$

where $\mathbf{\Psi}(\mathbf{X})$ contains the state-dependent lifted data. The closed-form solution follows from the associated normal equations, yielding the predictor (7) together with an output matrix $\mathbf{C}_z$ estimated analogously [4], [16].

The choice of $\mathbf{\Phi}$ is system-specific. For the TCLab, a predefined spectral dictionary ϕ_{vec} of nonlinear basis functions is employed. EDMD yields a complex-valued model of dimension 20×20; to enable real-time implementation, it is converted to a real-valued form by separating real and imaginary parts, giving $\mathbf{A}_z \in \mathbb{R}^{40\times 40}$.

For the multi-tank system, the dictionary combines polynomial state observables up to third order with input–state interaction terms:

$$\mathbf{\Phi}(\mathbf{x}, \mathbf{u}) = \left[\mathbf{\Psi}_1(\mathbf{x}) \ \ \mathbf{x} \otimes \mathbf{u}\right]^\top, \tag{21}$$

where $\mathbf{\Psi}_1(\mathbf{x})$ collects all monomials up to degree 3 and $\mathbf{x} \otimes \mathbf{u}$ captures pairwise products between states and inputs, essential for non-affine dynamics [4]. This yields $\mathbf{A}_z \in \mathbb{R}^{22\times 22}$, $\mathbf{B}_z \in \mathbb{R}^{22\times 3}$, $\mathbf{C}_z \in \mathbb{R}^{2\times 22}$.

To eliminate steady-state tracking error, the lifted model is augmented by appending the output error $\boldsymbol{\delta}_k = \mathbf{y}_k - \mathbf{C}_z \mathbf{z}_k$ to the state vector, giving $\tilde{\mathbf{z}}_k = [\mathbf{z}_k^\top \ \boldsymbol{\delta}_k^\top]^\top$. The augmented model embeds integral action and serves as the internal prediction model for the MPC.

Since $\mathbf{z}_k$ is not directly measurable, a state observer is required for the TCLab. The observer gain is computed via a discrete-time LQR problem on the lifted model, reconstructing $\hat{\mathbf{z}}_k$ from the measured temperatures. For the multi-tank system, $\mathbf{z}_k$ is evaluated analytically at each step as $\mathbf{\Phi}(\mathbf{x}_k, \mathbf{u}_k)$, making a dynamic observer unnecessary.

At each sampling instant the controller solves the QP defined by the cost (8) subject to (9), using prediction matrices built from the augmented lifted model [13]. For the TCLab: $T_s = 2\,\mathrm{s}$, $N_p = 21$, $N_c = 12$, penalty weights $\lambda_1 = 0.094456$ and $\lambda_2 = 0.022812$; the QP is solved via Hildreth's algorithm [4]. For the multi-tank system: $T_s = 1\,\mathrm{s}$, $N_p = 5$, with $0 \leq u_i \leq 1$ and $0 \leq h_i \leq 0.2\,\mathrm{m}$.

D. Comparison Setup

The comparison between SIMC-PID and Koopman-MPC was performed under equivalent reference trajectories, actuator constraints, and performance metrics. Step changes were applied to the TCLab temperature references and to the multi-tank level references.

In all cases, both the controlled variables and the corresponding control signals were analyzed. The error indices used were IAE, ITAE, and ISE, defined as

$$\mathrm{IAE} = \int_0^T |e(t)|\, dt, \tag{22}$$

$$\mathrm{ITAE} = \int_0^T t\, |e(t)|\, dt, \tag{23}$$

$$\mathrm{ISE} = \int_0^T e^2(t)\, dt, \tag{24}$$

where $e(t)$ represents the tracking error between the reference and the system output. For the multivariable systems considered (TCLab and multitank system), the error is defined individually for each controlled variable as

$$e_i(t) = r_i(t) - y_i(t), \quad i = 1, 2 \tag{25}$$

according to the pairings defined for each system.

The performance indices (IAE, ITAE, and ISE) were computed for each output and control strategy. A global index was then obtained by summing the individual output values, enabling both local and overall performance comparison between controllers.

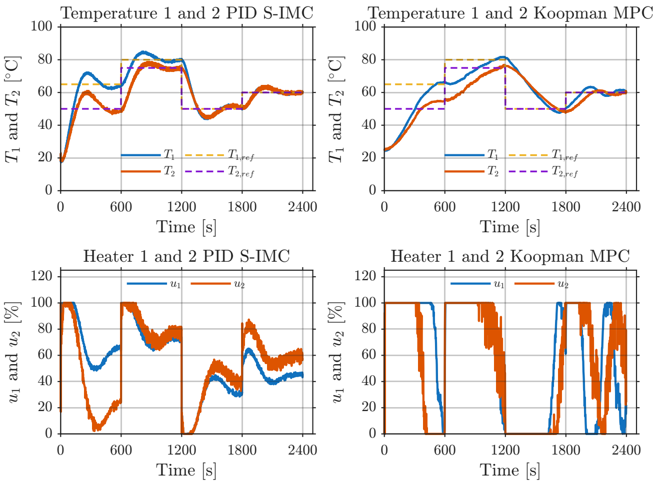

Fig. 1. TCLab MIMO response under PID S-IMC and Koopman MPC for four reference changes at sampling time of $T_s = 2\,\mathrm{s}$. Measured outputs and control inputs are shown.

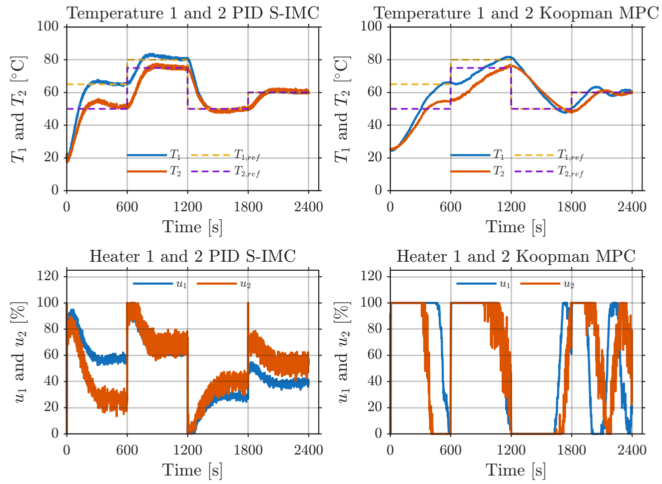

Fig. 2. TCLab MIMO response under PID S-IMC and Koopman MPC for four reference changes with $T_{s,\mathrm{PID}} = 1\,\mathrm{s}$ and $T_{s,\mathrm{MPC}} = 2\,\mathrm{s}$.

TABLE III

TCLab: IAE, ITAE, and ISE for PID vs. Koopman MPC in Experiment 1 using a 2 s sampling time for both controllers

	IAE		ITAE		ISE	
Output	PID	MPC	PID	MPC	PID	MPC
y_1	12802	23492	9.57×10^6	1.77×10^7	2.49×10^5	5.13×10^5
y_2	12241	20875	9.79×10^6	1.90×10^7	1.75×10^5	3.33×10^5
TOTAL	25043	44367	1.93×10^7	3.67×10^7	4.24×10^5	8.47×10^5

TABLE IV

TCLab: IAE, ITAE, and ISE for PID vs. Koopman MPC in Experiment 2 ($T_{s,\mathrm{PID}} = 1\,\mathrm{s}$, $T_{s,\mathrm{MPC}} = 2\,\mathrm{s}$)

	IAE		ITAE		ISE	
Output	PID	MPC	PID	MPC	PID	MPC
y_1	10754	23492	7.76×10^6	1.77×10^7	2.17×10^5	5.13×10^5
y_2	10478	20875	8.18×10^6	1.90×10^7	1.55×10^5	3.33×10^5
TOTAL	21232	44367	1.59×10^7	3.67×10^7	3.72×10^5	8.47×10^5

IV. Results

Fig. 1 shows the responses of the TCLab system under the action of the PID and MPC controllers. It can be observed that both strategies achieve reference tracking; however, there are differences in the dynamic behavior, particularly in the settling time and the smoothness of the response.

Table III presents the values of the performance indices IAE, ITAE, and ISE for both system outputs. It is observed that the PID controller presents lower values in all metrics, both individually and in the total value, which indicates better performance in terms of accuracy, response speed, and accumulated error of the system variables. These results show a more efficient response of the PID compared to the MPC in this scenario.

Fig. 2 presents the responses of the TCLab system for another study. In this case, a general improvement in the performance of both controllers is observed compared to the previous study, with faster responses and reduced oscillations. Table IV presents the values of the performance indices IAE, ITAE, and ISE for both system outputs. It is observed that the PID controller presents lower values in all metrics, both individually and in the total value, which confirms better performance in terms of accuracy, temporal response, and error energy compared to the MPC.

Fig. 3 shows the responses of the multi-tank system. Unlike the TCLab system, it is observed that the relative behavior between PI and MPC varies depending on the output considered, highlighting its coupled nature.

Table V presents the values of the performance indices for both system outputs. It is observed that the PI controller achieves lower total values in the IAE, ITAE, and ISE indices. However, the relative behavior varies depending on the output: the PI presents lower error in y_1, whereas the MPC achieves slightly lower values in y_2. These results show a trade-off between the individual output performance and the global behavior of both strategies.

TABLE V

Multi-tank: IAE, ITAE, and ISE for PI vs. Koopman MPC (four level setpoint changes)

	IAE		ITAE		ISE	
Output	PI	MPC	PI	MPC	PI	MPC
y_1	16.631	34.723	9890.9	13574	1.129	3.238
y_2	43.726	42.571	36433	32909	4.201	3.982
TOTAL	60.356	77.294	46324	46483	5.331	7.220

Beyond the error metrics, a consistent pattern emerges in the control effort. For the TCLab (Figs. 1–2), the PID produces smoother actuator signals, while the MPC exhibits more aggressive variations and frequent saturation, indicating that added algorithmic complexity does not translate into practical benefit when the system dynamics are simple. For the multi-tank system (Fig. 3), although the MPC improves the response of one output, the corresponding valve signals show prolonged saturation and abrupt switching, whereas the PI delivers smoother, lower-energy actuation reflected in its lower total ISE. Overall, these results support the conclusion that performance is jointly determined by method complexity and system characteristics, and that a well-designed classical controller remains a competitive alternative in scenarios with relatively simple or weakly coupled dynamics.

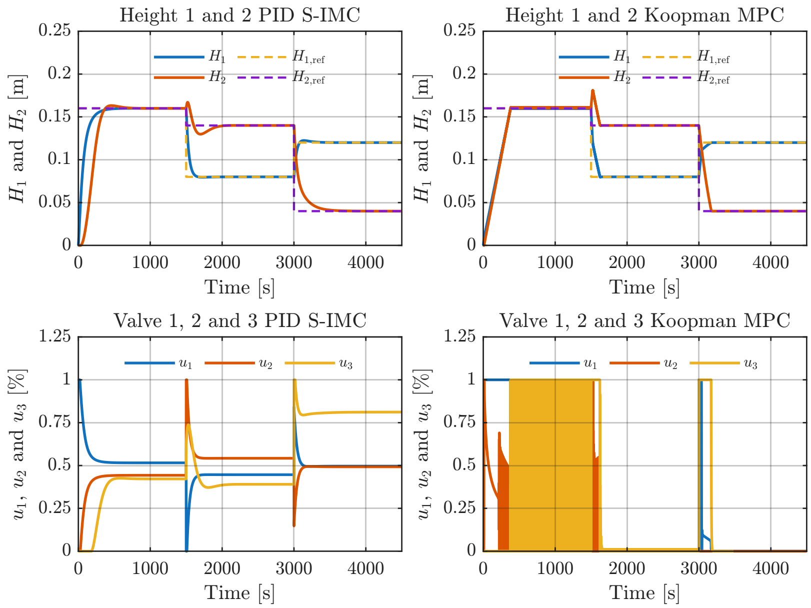

Fig. 3. Multi-tank MIMO responses under PI and Koopman MPC with four reference changes. Measured levels and control inputs are shown.

V. Conclusions

The results obtained throughout the different studies allow identifying clear trends in the performance of the analyzed controllers. In the TCLab system, the PID controller consistently presented lower values in the IAE, ITAE, and ISE indices, showing a more accurate and faster response with lower error accumulation compared to the MPC. This behavior suggests that, for systems with relatively simple dynamics and low coupling, classical control strategies can provide favorable results with lower implementation complexity.

In contrast, in the multi-tank system a different behavior was observed, where the MPC achieved better performance in terms of the IAE and ITAE indices, reflecting a greater capability to manage the error over time in systems with multiple interdependent variables. However, the PI maintained advantages in the ISE, indicating lower error energy and a smoother response under certain conditions.

Overall, these results show that the relative performance between PID and MPC is not uniform, but depends on the characteristics of the system, the control objectives, and the evaluation criteria considered. Therefore, this work does not state that one strategy is inherently better than the other. Instead, it highlights that the selection of a controller must depend on the specific application context. In many practical cases, making changes or adjustments to a PID controller is simpler, less computationally demanding, and can still lead to favorable results. This also helps explain why PID controllers continue to be widely used in industry, where simplicity, ease of tuning, robustness, and reliable performance remain important factors in control system implementation.

References

[1] Sigurd Skogestad. Advanced control using decomposition and simple elements. *Annual Reviews in Control*, 56, 1 2023.

[2] Sigurd Skogestad. Probably the best simple pid tuning rules in the world. In *AIChE Annual Meeting*, 11 2001.

[3] Ágnes Bárkányi, Tibor Chován, Sándor Németh, and János Abonyi. Modelling for digital twins—potential role of surrogate models. *Processes*, 9, 3 2021.

[4] Juan Francisco Durán-Siguenza, Luis Ismael Minchala, Luis E. Garza-Castañón, and Huiyan Zhang. Control based on the koopman operator: A comprehensive review. *Journal of the Franklin Institute*, 362, 12 2025.

[5] Pouria Sarhadi. On the standard performance criteria for applied control design: Pid, mpc or machine learning controller? *arXiv preprint arXiv:2503.14379*, 10 2025.

[6] E. Kaiser, J. N. Kutz, and S. L. Brunton. Sparse identification of nonlinear dynamics for model predictive control in the low-data limit. *Proceedings of the Royal Society A: Mathematical, Physical and Engineering Sciences*, 474, 11 2018.

[7] Andrew J. Taylor, Victor D. Dorobantu, Sarah Dean, Benjamin Recht, Yisong Yue, and Aaron D. Ames. Towards robust data-driven control synthesis for nonlinear systems with actuation uncertainty. In *2021 60th IEEE Conference on Decision and Control (CDC)*, pages 6469–6476. IEEE, 12 2021.

[8] Sigurd Skogestad and Ian Postlethwaite. *Multivariable Feedback Control. Analysis and Design*. John Wiley & Sons, Ltd, 2nd edition, 10 2005.

[9] Sigurd Skogestad. Simple analytic rules for model reduction and pid controller tuning. *Journal of Process Control*, 13:291–309, 6 2003.

[10] Sigurd Skogestad and Chriss Grimholt. *The SIMC Method for Smooth PID Controller Tuning*, pages 147–175. Springer, London, 2012.

[11] Steven L. Brunton and J. Nathan Kutz. *Data-Driven Science and Engineering: Machine Learning, Dynamical Systems, and Control*. Cambridge University Press, 2nd edition, 6 2022.

[12] Alexandre Mauroy and Jorge Goncalves. *Parameter Estimation and Identification of Nonlinear Systems with the Koopman Operator*, volume 484, pages 335–357. Springer, Cham, 2020.

[13] Liuping Wang. *Model Predictive Control System Design and Implementation Using MATLAB®*. Springer London, 2009.

[14] Mario Fernández. *Control del sistema TCLab con técnicas de control predictivo*. PhD thesis, Escuela Técnica Superior de Ingeniería Universidad de Sevilla, 2021.

[15] Galo Guzmán-Guillén, Luis A. Andrade, and Luis I. Minchala. Digital twin framework for multi-tank systems with opc ua interoperability and real-time control and visualization. In *2025 IEEE Ninth Ecuador Technical Chapters Meeting (ETCM)*, pages 1–6. IEEE, 10 2025.

[16] Ali Khaki-Sedigh. *An Introduction to Data-Driven Control Systems*. John Wiley&Sons, Inc., 1st edition, 12 2023.